



Experimental and theoretical DFT studies of structure, spectroscopic and fluorescence properties of a new imine oxime derivative

Yunus Kaya^a, Veysel T. Yilmaz^{a,*}, Taner Arslan^b, Orhan Buyukgungor^c

^a Department of Chemistry, Faculty of Arts and Sciences, Uludag University, 16059 Bursa, Turkey

^b Department of Chemistry, Faculty of Arts and Sciences, Eskisehir Osmangazi University, 26480 Eskisehir, Turkey

^c Department of Physics, Faculty of Arts and Sciences, Ondokuz Mayıs University, 55139 Samsun, Turkey

HIGHLIGHTS

- ▶ (1*E*,2*E*)-phenyl-[(1-phenylethyl)imino]-ethanal oxime was synthesized and characterized by IR, UV–vis, NMR and X-ray crystallography.
- ▶ The structure of the title compound is stabilized by intermolecular O–H···N hydrogen bonds.
- ▶ Molecular geometry and conformations were determined by DFT method.
- ▶ The compound in DMSO is fluorescent at room temperature.

ARTICLE INFO

Article history:

Received 28 March 2012
 Received in revised form 8 May 2012
 Accepted 9 May 2012
 Available online 17 May 2012

Keywords:

Oxime
 X-ray structure
 DFT calculations
 Isomerization
 Spectroscopy
 Photoluminescence

ABSTRACT

A new imine oxime, (1*E*,2*E*)-phenyl-[(1-phenylethyl)imino]-ethanal oxime (**I**), is synthesized and characterized. The title compound crystallizes in the monoclinic space group $P2_1/c$ with $a = 12.3416(7)$, $b = 9.5990(6)$, $c = 11.9750(7)$, $\beta = 92.417(4)$ and $Z = 4$. Crystallographic, vibrational (IR), and NMR (^1H and ^{13}C chemical shifts) data are compared with the results of density functional theory (DFT) method at the B3LYP/6-311++G(d,p) level. The structure of **I** is stabilized by intermolecular O–H···N hydrogen bonds. The theoretical calculations show that the compound exhibits a number of isomers, and the molecular geometry of the most stable optimized isomer (*s-trans-E,E*) can well reproduce the X-ray structure. The calculated vibrational bands and NMR chemical shifts are consistent with the experimental results. The NBO/NPA atomic charges are performed to explore the possible coordination modes of the compound. The electronic (UV–vis) and photoluminescence spectra calculated using the TD-DFT method are correlated to the experimental spectra. The DMSO solutions of **I** are fluorescent at room temperature. The assignment and analysis of the frontier HOMO and LUMO orbitals indicates that both absorption and emission bands are originated mainly from the π – π^* transitions.

© 2012 Elsevier B.V. All rights reserved.

1. Introduction

The syntheses, structural properties, analytical applications, solution and coordination chemistry of oximes and their metal complexes have been extensively studied and described in great detail [1–7]. Oximes as ligands played a significant role in the development of transition metal chemistry. Since the oxime group possesses two potential coordinating donor sites such as the nitrogen and oxygen atoms, these compounds usually exhibit an ambidentate coordination behavior. However, in most cases, the coordination occurs via the nitrogen atom. Some oximes showed versatile antimicrobial activity [8–10], while some platinum(II) complexes of oximes exhibited high DNA binding affinity as well as significant cytotoxic activity [11–14].

The imine–oximes are Schiff bases of carbonyl–oximes, usually acting as bidentate ligands through the oxime and imine nitrogen atoms. Upon complexation, the oxime hydrogen may or may not dissociate. It was suggested that the coordination geometry of the simple imine–oximes in metal complexes of the type $[\text{M}(\text{L})_2]$ ($\text{M} = \text{Co}^{\text{II}}$, Ni^{II} and Cu^{II}) is *trans*-square-planar, but the octahedral geometry occurs in the case of additional ligands such as Cl, I and SCN at axial positions [1].

Due to broad interest in oximes, their structure, reactivity and metal complexing capability have been investigated and well documented in the literature [1–7]. Furthermore, the theoretical studies on isomerizations [15–28], reaction mechanisms [29–32] and spectroscopic characteristics (UV–vis, IR, Raman and NMR) [33–41] of some oximes were also performed. However, to the best of our knowledge, no theoretical study was present on the imine–oximes. The aim of this work is to study the molecular structure, possible isomers and spectroscopic characterization of a new

* Corresponding author.

E-mail address: vtyilmaz@uludag.edu.tr (V.T. Yilmaz).

imine-oxime, namely (1*E*,2*E*)-phenyl-[(1-phenylethyl)imino]-ethanal oxime (**1**). For this purpose, density functional theory (DFT) calculations were performed to explain the structural and spectral characteristics of the compound. Molecular structure parameters, vibrational frequencies and NMR chemical shifts of the title compound have been calculated by B3LYP/6-311++G(d,p) level of theory and compared with the experimental data. HOMO, LUMO and UV spectral analysis have been used to elucidate the electronic transitions within the molecule. In addition, the photoluminescence properties of the compound were investigated.

2. Experimental

2.1. Materials and measurements

All reagents used for the synthesis of the compound are commercially available and were used without further purification. Elemental analyses for C, H, and N were performed using a EuroEA 3000 CHNS elemental analyser. UV–vis spectra were measured on a Perkin-Elmer Lambda 35 UV/vis spectrophotometer using 1×10^{-5} M EtOH solutions in the 200–800 nm range. IR spectra were recorded on a Thermo Nicolet 6700 FT-IR spectrophotometer as KBr pellets in the frequency range 4000–400 cm^{-1} . ^1H NMR and ^{13}C NMR spectra were recorded on a Varian Mercuryplus spectrometer. Excitation and emission spectra of 1×10^{-3} M DMSO solutions were recorded at room temperature with a Varian Cary Eclipse spectrophotometer equipped with a Xe pulse lamp of 75 kW.

2.2. Synthesis

1-Phenylethylamine (0.61 g, 5 mmol) dissolved in 5 mL EtOH was added dropwise in a 10 mL EtOH solution of isonitrosoacetophenone (0.75 g, 5 mmol) and the resulting solution was stirred at room temperature for 3 h. Well-shaped prisms of **1** were obtained by slow evaporation at room temperature within 3 days. Yield 61%. Mp. 136 °C. Anal. Calcd. $\text{C}_{16}\text{H}_{16}\text{N}_2\text{O}$: C, 76.16; H, 6.34; N, 11.10. Found: C, 76.36; H, 6.29; N, 10.98.

2.3. X-ray crystallography

The intensity data of **1** were collected using a STOE IPDS 2 diffractometer with graphite-monochromated Mo $K\alpha$ radiation ($\lambda = 0.71073$ Å). The structures were solved by direct methods and refined on F^2 with the SHELX-97 program [42]. All non-hydrogen atoms were found from the difference Fourier map and refined anisotropically. Hydrogen atoms bonded to C atoms were refined using a riding model, while the hydroxyl hydrogen atom is refined freely. The details of data collection, refinement and crystallographic data are summarized in Table 1.

2.4. Theoretical methods

All the calculations are performed by using GAUSSVIEW molecular visualization program [43] and GAUSSIAN 03 program package [44]. The calculations have been carried out at DFT using the hybrid B3LYP approach [45] and the 6-311++G(d,p) basis set. The vibrational frequencies of the molecule were carried out for the complete equilibrium geometry obtained by the same quantum chemical model in the gas phase. The frequency values computed at these levels contain known systematic errors and therefore, scaling factors 0.958 [46] and 0.978 [47] were used for 4000–1700 cm^{-1} and 1700–400 cm^{-1} ranges, respectively. ^1H and ^{13}C NMR chemical shifts of the compound were calculated using the GIAO method [48] in DMSO- d_6 and TMS as a reference.

Table 1
Crystallographic data and structure refinement for compound **1**.

	1
Formula	$\text{C}_{16}\text{H}_{16}\text{N}_2\text{O}$
Molecular weight	252.31
Temperature	298(2)
Wavelength	0.71073 Å
Crystal system	Monoclinic
Space group	$P2_1/c$
Unit cell dimensions	
<i>a</i> (Å)	12.3416(7)
<i>b</i> (Å)	9.5990(6)
<i>c</i> (Å)	11.9750(7)
β (°)	92.417(4)
Volume (Å ³)	1417.38(15)
<i>Z</i>	4
Calculated density (g/cm ³)	1.182
μ (mm ⁻¹)	0.075
<i>F</i> (000)	536
θ Range (°)	1.65–28.03
Index ranges	$-15 \leq h \leq 15$, $-12 \leq k \leq 12$, $-14 \leq l \leq 14$
Reflections collected	12,659
Independent reflections	2932 [$R_{\text{int}} = 0.0281$]
Reflections observed ($>2\sigma$)	2124
Absorption correction	Integration
Max. and min. transmissions	0.9891 and 0.9513
Data/parameters	2932/177
Goodness-of-fit on F^2	1.0659
Final <i>R</i> indices [$I > 2\sigma(I)$]	$R_1 = 0.0395$ $wR_1 = 0.1054$
Largest diff. peak and hole ($\text{e} \text{ \AA}^{-3}$)	0.106 and -0.108

The absorption spectra of the complexes in EtOH were calculated based on the optimized singlet-states using restricted time-dependent DFT (TD-DFT) with the Polarizable Continuum Model (PCM) using the integral equation formalism variant (IEFPCM) at the B3LYP/LanL2DZ level, while the optimized triplet excited-states were used for the emission spectral analysis, using unrestricted time-dependent DFT (TD-DFT). GaussSum was used to calculate group contributions to the molecular orbitals and to simulate the UV–vis absorption and fluorescence emission spectra [49].

3. Results and discussion

3.1. Description of the crystal structure

The molecular structure of **1** is shown in Fig. 1, and the bond lengths and angles are given in Table 2. The compound crystallizes in the monoclinic space group $P2_1/c$ with four molecules in the unit cell. The title compound is chiral and the crystal structure contains both enantiomers. Compound **1** not planar and the overall molecular conformation can readily be defined in terms of the torsion angles. As expected, the phenyl moieties are planar and almost perpendicular to each other with a dihedral angle of 89.44(3)°. The C9–N1–C7 unit combining both phenyl groups has a angle of 121.05(10)°. The bond distances in Table 2 show that the double bonds in the molecule are localized between the C9 and N1, and C10 and N2 atoms, resulting in bond lengths of 1.2797(15) and 1.2747 Å, respectively, which are significantly shorter than the C7–N1 single bond with a length of 1.4695(16) Å. The C=N bond distances in the title compound are comparable to the corresponding bonds found in the similar oxime derivatives [50,51]. The molecules of **1** are linked by O–H...N (symmetry code: $-x + 1, y + 1/2, -z + 1/2$) intermolecular hydrogen bonds involving the hydroxyl hydrogen atom and the imine N atom. The hydrogen bonds result in a one-dimensional chain running along the *b* axis and these chains are held together by van der Waals interactions forming a three-dimensional network.

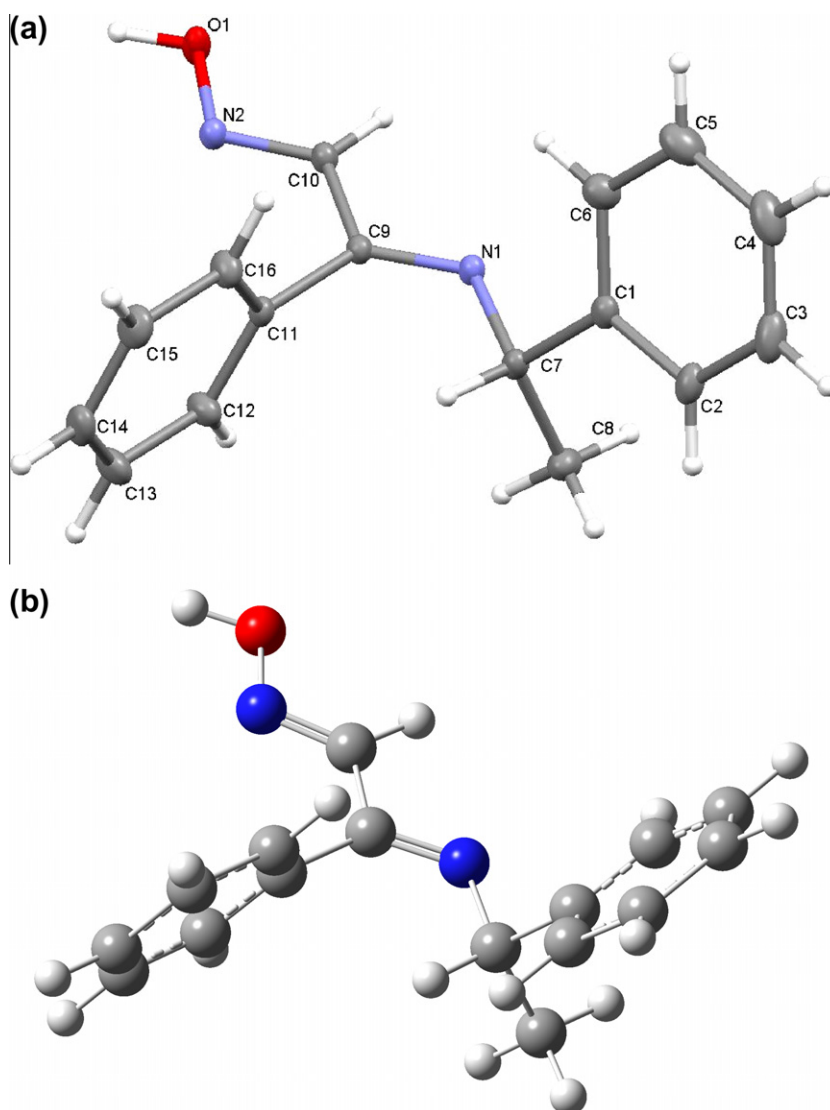


Fig. 1. Molecular view of compound I. (a) X-ray structure and (b) optimized structure of the *trans-E,E* isomer.

3.2. Isomerization and optimized geometry

The oximes show geometrical isomerism due to rotation of the C=N bond. The structure of I is very flexible and represents several conformations as illustrated in Fig. 2. To establish the most stable conformation, the molecule was subjected to a rigorous conformation analysis around the free rotation bonds. Since the calculated dihedral angles between the planes of the double bonds in Table 3 clearly indicate that they are not coplanar in the calculated structures, the *cis* and *trans* conformations of *E*- and *Z*-isomers can more appropriately be called as *s-cis* (*cisoid*) and *s-trans* (*transoid*) [52,53]. The energies of the studied isomers are listed in Table 3. In the gas phase, the *s-trans-E,E* isomer is the most stable one, while the *s-trans-Z,Z* isomer is the less stable. The other isomers (*s-cis-E,E*, *s-cis-Z,Z* and *s-E,Z*) lie between the *s-trans-E,E* and *s-trans-Z,Z* isomers. These findings agree well with the reported results on the isomerization of oximes [15,20,54,55]. The molecular geometries of the most stable isomer (*s-trans-E,E*) and the title compound shows conformational discrepancies. The most notable mismatch is observed in the orientation of the phenyl rings. The experimental dihedral angle between these rings is $89.44(3)^\circ$, whereas it was calculated as $28.58(2)^\circ$ for the *s-trans-E,E* isomer. The present

discrepancy mainly arises from a rotation around the C1–C7 bond. The calculated dipole moments of the isomers of title compound are also presented in Table 3. It should be noted that the dipole moments are very much sensitive to the conformation of the isomers.

3.3. Atomic charges

The NBO/NPA atomic charges [56,57] were calculated using the B3LYP/6-311G++(d,p) base set. The results are listed in Table 4. Most of the carbon atoms, except the C9 and C10 atoms, contain negative charges and the NBO charges on the carbon atoms range from -0.029 to -0.556 atomic charge unit (a.c.h.u.). However, the methyl carbon atom (C8) is the most negative carbon atom. The C9 and C10 atoms to the N atoms have positive charges of 0.231 and 0.033, respectively. Both N atoms have negative charges, but the N1 atom is much more negative the imine N atom (N2), suggesting it as a possible donor to metal ions. On the other hand, the O atom of the hydroxyl group have a significant negative charge (-0.548 a.c.h.u.) and the O atom also serves as another coordinating site to metal ions. The NBO charges clearly indicate that the title compound can act as a bidentate ligand through the N1 and hydroxyl O atoms.

Table 2
Geometric parameters of compound **I**.

Parameter	X-ray	B3LYP/6-311++G(d,p)
<i>Bond length (Å)</i>		
C1–C2	1.385(19)	1.397
C2–C3	1.379(3)	1.395
C3–C4	1.356(3)	1.393
C4–C5	1.384(4)	1.395
C5–C6	1.388(3)	1.394
C1–C6	1.378(2)	1.399
C1–C7	1.512(2)	1.525
C7–C8	1.521(2)	1.541
C9–C10	1.461(17)	1.476
C9–C11	1.494(16)	1.502
C11–C12	1.367(2)	1.398
C12–C13	1.382(2)	1.393
C13–C14	1.351(3)	1.394
C14–C15	1.363(3)	1.394
C15–C16	1.388(2)	1.394
C11–C16	1.371(2)	1.399
C7–N1	1.470(16)	1.461
C9–N1	1.280(15)	1.280
C10–N2	1.275(15)	1.276
N2–O1	1.382(13)	1.396
O1–H	0.890(2)	0.964
<i>Bond angle (°)</i>		
C1–C2–C3	121.1(19)	120.8
C2–C1–C7	120.8(14)	119.8
C2–C3–C4	120.6(19)	120.1
C3–C4–C5	119.6(2)	119.5
C4–C5–C6	119.6(2)	120.3
C6–C1–C7	121.3(13)	121.4
C6–C1–C2	117.8(15)	118.7
C1–C6–C5	121.1(19)	120.5
N1–C7–C1	109.6(11)	109.7
N1–C7–C8	106.6(12)	107.8
C1–C7–C8	114.7(11)	111.3
C9–N1–C7	121.1(10)	121.8
N1–C9–C10	117.0(10)	114.9
N1–C9–C11	125.1(11)	126.6
C10–C9–C11	117.9(10)	118.4
C9–C10–N2	118.9(10)	120.9
C12–C11–C16	119.3(12)	119.2
C12–C11–C9	120.9(12)	120.5
C16–C11–C9	119.9(12)	120.3
C11–C12–C13	120.5(16)	120.4
C12–C13–C14	120.1(18)	120.2
C13–C14–C15	120.3(15)	119.7
C14–C15–C16	120.0(17)	120.2
C11–C16–C15	119.9(16)	120.4
C10–N2–O1	111.4(10)	111.3

3.4. Vibrational spectra

Table 5 lists the experimentally observed FTIR bands of compound **I** and the most intense vibrational frequencies calculated by the DFT method at the B3LYP/6-311++G(d,p) level together with their main mode contributions. The calculated frequencies with the intensity less than 5 were not taken into consideration. The vibrations below ca. 1450 cm⁻¹ are very complex and involve several coupled motions. In general, comparison of the experimental IR bands and those obtained by the DFT method shows overall good agreement as evident from inspection of Table 5. The band centered at 3241 cm⁻¹ corresponds to the vibration of the hydroxyl group, which participates to strong hydrogen bonding in the crystalline state as discussed above. The hydrogen bonding is important for the stabilization of oximes [58] and the calculations showed that a hydrogen bonded dimer of the title compound has lower energy (-29.5 kJ mol⁻¹) compared to the single molecule. In the present case, the difference between the experimental and calculated values is 420 cm⁻¹. The calculated aromatic and aliphatic C–H vibrations were found in the range of 3060–2890 cm⁻¹, in agreement with

the experimental values. The experimental C=N bands were observed at 1612 and 1597 cm⁻¹ as sharp bands and the calculated values of this mode were somewhat shifted to the higher frequency appearing at 1646 and 1629 cm⁻¹. The calculated C=C stretching band of the phenyl rings at 1606 cm⁻¹ was practically not observed experimentally. However, their $\delta(\text{C}=\text{C})$ and $\delta(\text{C}=\text{C})$ modes occurred at 1022 and 704 cm⁻¹ as coupled with other vibrational modes of **I**. In addition, the C–C stretching vibrations were observed at 1069 and 1022 cm⁻¹, and calculated at 1092 and 998 cm⁻¹. Although the calculated vibrational frequencies in some cases significantly deviate from the experiment, the correlation is very linear ($r^2 = 0.9954$).

3.5. NMR spectra

Experimental and calculated ¹H and ¹³C NMR spectra in DMSO-*d*₆ with TMS as a reference are illustrated in Fig. 3 and the chemical shifts are given in Table 6. The numbering of the atoms is the same as in Fig. 1. As can be seen from Table 6, the NMR shifts obtained by the DFT method at the B3LYP/6-311++G(d,p) level are in reasonable agreement with the experimental values of the ¹³C NMR spectrum. The ¹H NMR spectrum is not well correlated with the calculated spectrum, since calculations are referred to the static molecule [59,60]. The deuterium exchangeable proton of the hydroxyimino group (–C=N–OH) shows a characteristic chemical shift at 11.79 ppm as singlet. The protons of the methyl group give a doublet at 1.32 ppm. The multiple peaks between 7.10 and 7.22 ppm represent the aromatic protons of the phenyl group (C2–C6), while the other phenyl group (C12–C16) is less shielded, giving chemical shifts in the range of 7.26–7.44 ppm. On the other hand, the C10–H proton is observed as a singlet at 7.88 ppm and the C7–H signal appears at 4.43–4.48 ppm as a quartet.

¹³C NMR spectrum shows 9 different carbon atoms. The signal at 164.27 ppm belongs to the C9 carbon atom and was calculated at 172.69 ppm. The carbon resonance of the C=N–OH group occurs at 152.63 ppm as expected for imine oximes [61,62] and was calculated as 162.89 ppm. The signals between 128.72 and 145.13 ppm are assigned to both phenyl carbon atoms and compare well with the calculated values. The C7 and C8 resonances are observed at 60.74 and 24.63 ppm, respectively and were calculated at 69.87 and 27.67 ppm, respectively.

3.6. UV–vis and photoluminescence spectra

Electronic absorption spectrum of compound **I** was studied in EtOH using the TD-DFT. Singlet excited states were calculated to predict the transition energies. The electronic transitions, oscillator strengths and their assignments are given in Table 7. The title compound displays a main absorption band centered at 236 nm ($\epsilon = 32,100 \text{ dm}^3 \text{ mol}^{-1} \text{ cm}^{-1}$). However, the calculated spectrum shows two absorption bands at 235 and 276 nm. The latter was not observed experimentally. The assignment of the calculated orbital excitations to the experimental bands was based on an overview of the contour plots and relative energy of occupied (HOMO) and unoccupied (LUMO) molecular orbitals involved in the electronic transitions (Fig. 4). The HOMO orbital is mainly located on one of the phenyl side, while the HOMO-4 orbital is localized on the C=N and OH groups as well as one of the phenyl ring. The LUMO orbital lies on the C=N and OH groups. The HOMO and LUMO orbitals have a π character and the experimental absorption band at 236 nm can be ascribed to the $\pi \rightarrow \pi^*$ transition between HOMO-4 and LUMO at 235 nm with an oscillator strength of 0.72.

The title compound is fluorescent in DMSO solutions upon excitation at room temperature. The room temperature emission spectra of **I** are presented in Fig. 5. When the title compound is excited at 298 nm, it fluoresces at 355 nm. On the other hand, the

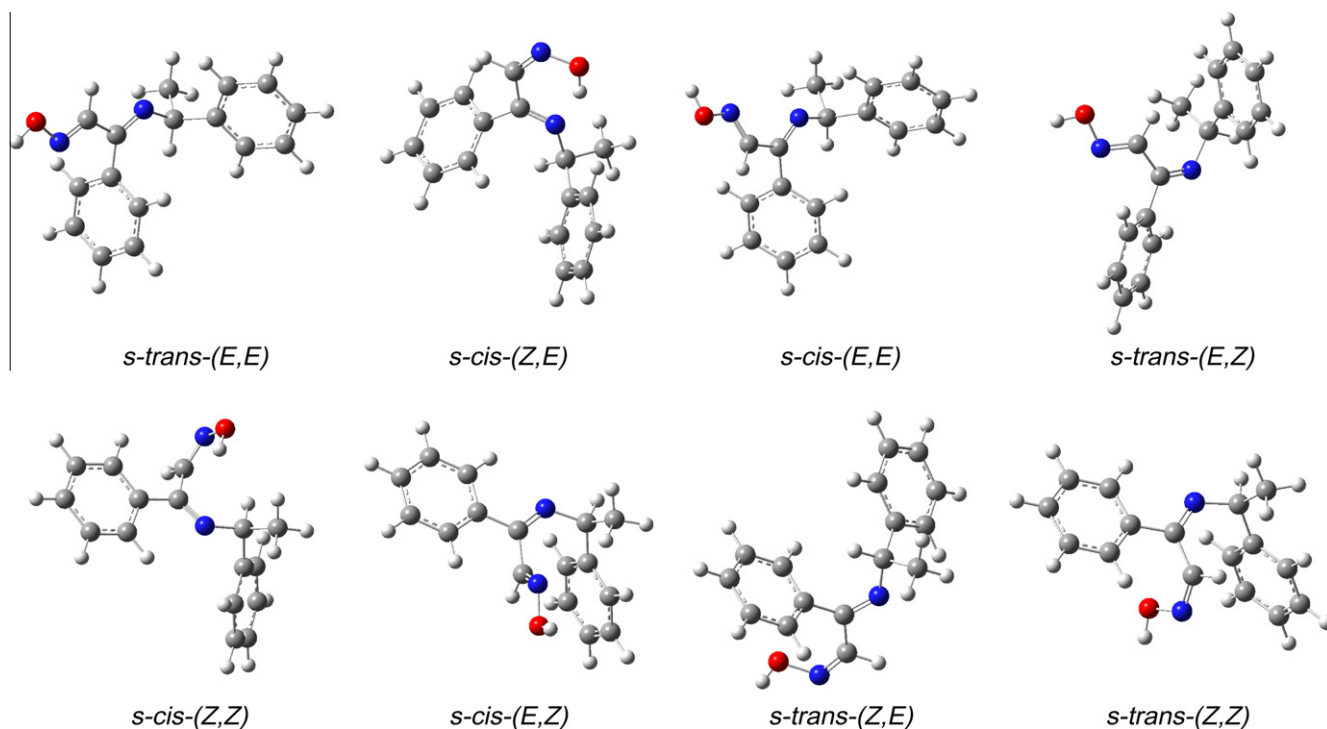


Fig. 2. The optimized geometries of all isomers of compound I.

Table 3
Calculated dihedral angles, energies and dipole moments of the isomers of compound I.

Isomers	Dihedral angles (N1=C9/C10=N2)		<i>E</i> (a.u.)	ΔE (kJ/mol)	μ (D)	
<i>s-trans</i>	<i>E</i>	<i>E</i>	−178.5	−804.2077	0.000	1.9123
<i>s-cis</i>	<i>Z</i>	<i>E</i>	2.3	−804.2074	0.786	5.5861
<i>s-cis</i>	<i>E</i>	<i>E</i>	34.4	−804.2007	18.375	2.0893
<i>s-trans</i>	<i>E</i>	<i>Z</i>	152.2	−804.1971	27.826	1.2855
<i>s-cis</i>	<i>Z</i>	<i>Z</i>	−77.0	−804.1962	30.188	2.8763
<i>s-cis</i>	<i>E</i>	<i>Z</i>	87.8	−804.1961	30.451	0.9201
<i>s-trans</i>	<i>Z</i>	<i>E</i>	−167.9	−804.1933	37.741	4.9202
<i>s-trans</i>	<i>Z</i>	<i>Z</i>	−118.4	−804.1930	38.557	0.9298

Table 4
Atomic charges of I.^a

Atom	NBO
C1	−0.029
C2	−0.196
C3	−0.196
C4	−0.208
C5	−0.199
C6	−0.204
C7	−0.067
C8	−0.556
C9	0.231
C10	0.033
C11	−0.101
C12	−0.176
C13	−0.196
C14	−0.199
C15	−0.197
C16	−0.188
N1	−0.424
N2	−0.122
O1	−0.548

^a Atomic charge units.

Table 5
Experimental and calculated IR spectral data^a of I together with their assignment.^b

Assignment	Experimental (cm ^{−1})	B3LYP/6-311++G(d,p)		
		Unscaled	Scaled	Intensity
$\nu(\text{O—H})$	3241m	3823	3662	150
$\nu(\text{C—H})_{\text{ring1}}$	3084m	3194	3060	12
$\nu(\text{C—H})_{\text{ring2}}$	3051w	3192	3058	7
$\nu(\text{C—H})_{\text{ring1}}$	3040w	3184	3050	26
$\nu(\text{C—H})_{\text{ring2}}$	3026m	3172	3039	23
$\nu(\text{C—H})_{\text{CHNOH}}$	2974m	3125	2994	6
$\nu(\text{C—H})_{\text{CH}_3}$ asym., $\nu(\text{C—H})_{\text{NCHCH}_3}$	2931w	3110	2979	16
$\nu(\text{C—H})_{\text{CH}_3}$ asym.		3099	2969	34
$\nu(\text{C—H})_{\text{CH}_3}$ sym.	2898m	3030	2903	26
$\nu(\text{C—H})_{\text{NCHCH}_3}$	2872m	3021	2894	18
$\nu(\text{C=N})$	1612s	1683	1646	7
$\nu(\text{C=N})$	1597s	1666	1629	91
$\nu(\text{C=C})_{\text{ring1}}$		1642	1606	8
$\delta(\text{C—H})_{\text{ring2}}$	1494s	1524	1490	13
$\gamma(\text{C—H})_{\text{CH}_3}$	1445w	1487	1454	6
$\gamma(\text{C—H})_{\text{CH}_3}$, $\delta(\text{C—H})_{\text{ring1}}$	1420w	1482	1449	7
$\delta(\text{O—H})$, $\delta(\text{C—H})_{\text{CHNOH}}$	1374w	1428	1397	64
$\delta(\text{C—H})_{\text{ring2}}$, $\gamma(\text{C—H})_{\text{NCHCH}_3}$, $\rho_r(\text{C—H})_{\text{CH}_3}$	1320w	1387	1356	22
$\delta(\text{C—H})_{\text{ring2}}$, $\gamma(\text{C—H})_{\text{NCHCH}_3}$, $\rho_r(\text{C—H})_{\text{CH}_3}$	1303m	1357	1327	10

excitation at 378 nm gives an emission band with three maximum at 439 nm. This band contains two maxima with a low intensity at

(continued on next page)

Table 5 (continued)

Assignment	Experimental (cm ⁻¹)	B3LYP/6-311++G(d,p)		
		Unscaled	Scaled	Intensity
$\gamma(\text{C-H})_{\text{NCHCH}_3}$, $\gamma(\text{C-H})_{\text{CH}_3}$, $\delta(\text{C-H})_{\text{ring2}}$, $\delta(\text{O-H})$	1273m	1312	1283	8
$\delta(\text{O-H})$, $\delta(\text{C-H})_{\text{CHNOH}}$		1266	1238	54
$\delta(\text{O-H})$, $\delta(\text{C-H})_{\text{CHNOH}}$, $\nu(\text{C-C})$, $\delta(\text{C-H})_{\text{ring1,2}}$	1069m	1117	1092	19
$\nu(\text{N-O})$, $\nu(\text{C-C})$, $\nu(\text{C-N})$, $\delta(\text{C=C})_{\text{ring1}}$	1022s	1020	998	33
$\rho_r(\text{C-H})_{\text{CH}_3}$, $\delta(\text{C=C})_{\text{ring1,2}}$		1002	980	7
$\rho_r(\text{C-H})_{\text{CH}_3}$, $\delta(\text{C-H})_{\text{ring1,2}}$, $\nu(\text{N-O})$	999s	991	969	171
$\gamma(\text{C-H})_{\text{CHNOH}}$	918m	979	957	10
$\rho_r(\text{C-H})_{\text{CH}_3}$, $\gamma(\text{C-H})_{\text{ring1}}$, $\gamma(\text{C-H})_{\text{ring2}}$	898m	911	891	17
$\gamma(\text{C-H})_{\text{ring1}}$	782w	821	803	12
$\gamma(\text{C-H})_{\text{ring2}}$	755w	788	771	5
$\rho_r(\text{C-H})_{\text{CH}_3}$, $\gamma(\text{C-H})_{\text{CHNOH}}$, $\delta(\text{C=C})_{\text{ring1,2}}$	704m	758	741	8
$\gamma(\text{C-H})_{\text{ring2}}$	695s	719	703	15
$\gamma(\text{C-H})_{\text{ring1}}$	684s	713	697	100
$\gamma(\text{C-H})_{\text{ring2}}$	679w	712	696	13
$\gamma(\text{C-H})_{\text{ring1}}$	669w	694	679	24
$\delta(\text{C=C})_{\text{ring2}}$, $\delta(\text{C=C})_{\text{ring1}}$	573m	621	607	11
$\delta(\text{C=C})_{\text{ring2}}$, $\delta(\text{C=C})_{\text{ring1}}$	540w	581	568	17
$\gamma(\text{C=C})_{\text{ring2}}$	523vw	558	546	21
$\gamma(\text{C=C})_{\text{ring1}}$	489vw	502	491	5
$\rho_r(\text{O-H})$	406w	443	433	112

^a w = weak, vw = very weak, s = strong, m = medium.

^b ν = stretching, δ = in-plane bending, γ = out-of-plane bending, ρ_r = rocking, asym = anti-symmetric, sym = symmetric, ring1 = C1–C6, ring2 = C11–C16.

Table 6

Experimental and calculated ¹H and ¹³C NMR chemical shifts (ppm).^a

Atom	Experimental	B3LYP/6-311++G(d,p)
¹ H NMR		
O1–H	11.79 s	8.09
C10–H	7.88 s	8.39
C13–H	7.44–7.26 m	7.79
C14–H		7.77
C15–H		7.72
C12–H		7.52
C16–H		7.15
C3–H	7.22–7.10 m	7.61
C4–H		7.60
C5–H		7.91
C2–H		7.00
C6–H		8.42
C7–H	4.45 m	4.25
C8–H	1.32 d	0.93–1.62
¹³ C NMR		
C9	164.27	172.69
C10	152.63	162.89
C1	145.13	153.89
C11	135.11	143.10
C12	128.80	134.02
C5	127.81	133.72
C16	128.80	133.44
C14	126.93	133.33
C6	128.72	133.33
C3	127.81	133.26
C13	127.68	133.01
C15	127.68	132.47
C4	126.93	132.02
C2	128.72	131.77
C7	60.74	69.87
C8	24.63	27.67

^a In DMSO-*d*₆ with TMS as a reference.

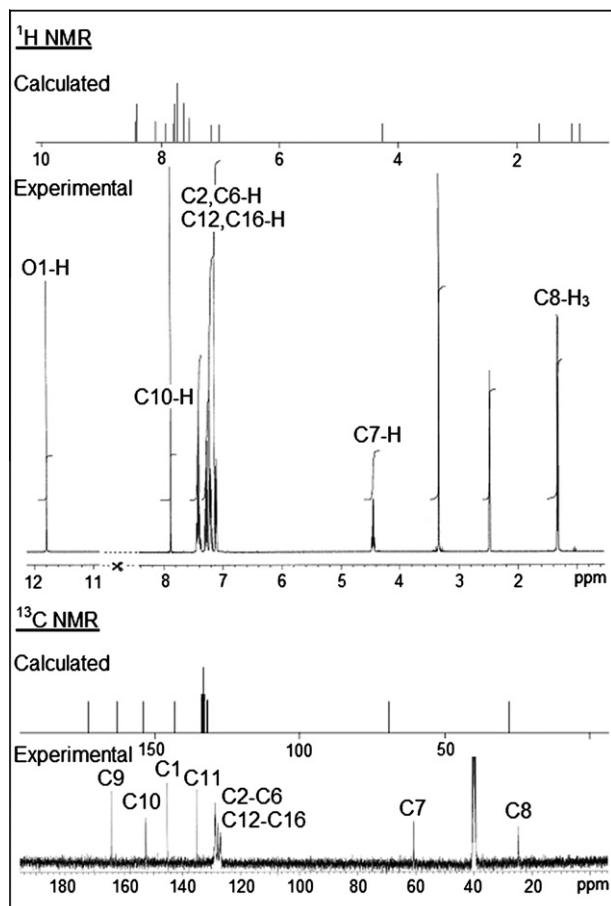


Fig. 3. Experimental and calculated NMR spectra of compound I.

Table 7

Experimental and calculated electronic transitions, oscillator strengths and their assignments for compound I.^a

Major contribution	Character	Calculated λ (nm), ΔE (eV), f_{os}	Experimental λ (nm), ΔE (eV), ϵ
<i>Absorption</i>			
H-4 → L (36%)	$\pi \rightarrow \pi^*$	235 5.29 0.72	236 5.26 32,100
H → L (74%)	$\pi \rightarrow \pi^*$	276 4.50 0.03	–
<i>Emission</i>			
H-8 β → L β (61%)	$\pi \rightarrow \pi^*$	339 3.66 0.13	355 ^b 3.50 –
H α → L α (78%)	$\pi \rightarrow \pi^*$	443 2.80 0.08	439 ^c 2.83 –

^a ϵ = Molar absorption coefficient (dm³ mol⁻¹ cm⁻¹), f_{os} = oscillator strength, H = highest occupied molecular orbital, L = lowest unoccupied molecular orbital.

^b Excited at 298 nm.

^c Excited at 378 nm.

416 and 464 nm. Again, α - and β -spin molecular orbitals involved in the transitions of the emission spectra have π character (Fig. 4). The emissions observed at 355 and 439 nm are related to the triplet state HOMO-8(β) → LUMO(β) and HOMO(α) → LUMO(α) transitions at 339 and 443 nm, respectively (Table 7). The energies of both emissions are in good agreement with the π - π^* transitions of the calculated spectra.

4. Conclusions

(1*E*,2*E*)-phenyl-[(1-phenylethyl)imino]-ethanal oxime is synthesized and characterized by elemental analysis, UV-vis, IR, ¹H NMR, ¹³C NMR and X-ray diffraction. Molecular geometries, electronic structures, vibrational and NMR, spectra of the title compound were investigated using the DFT method. The TD-DFT calculations in the solution (EtOH and DMSO) were used to predict

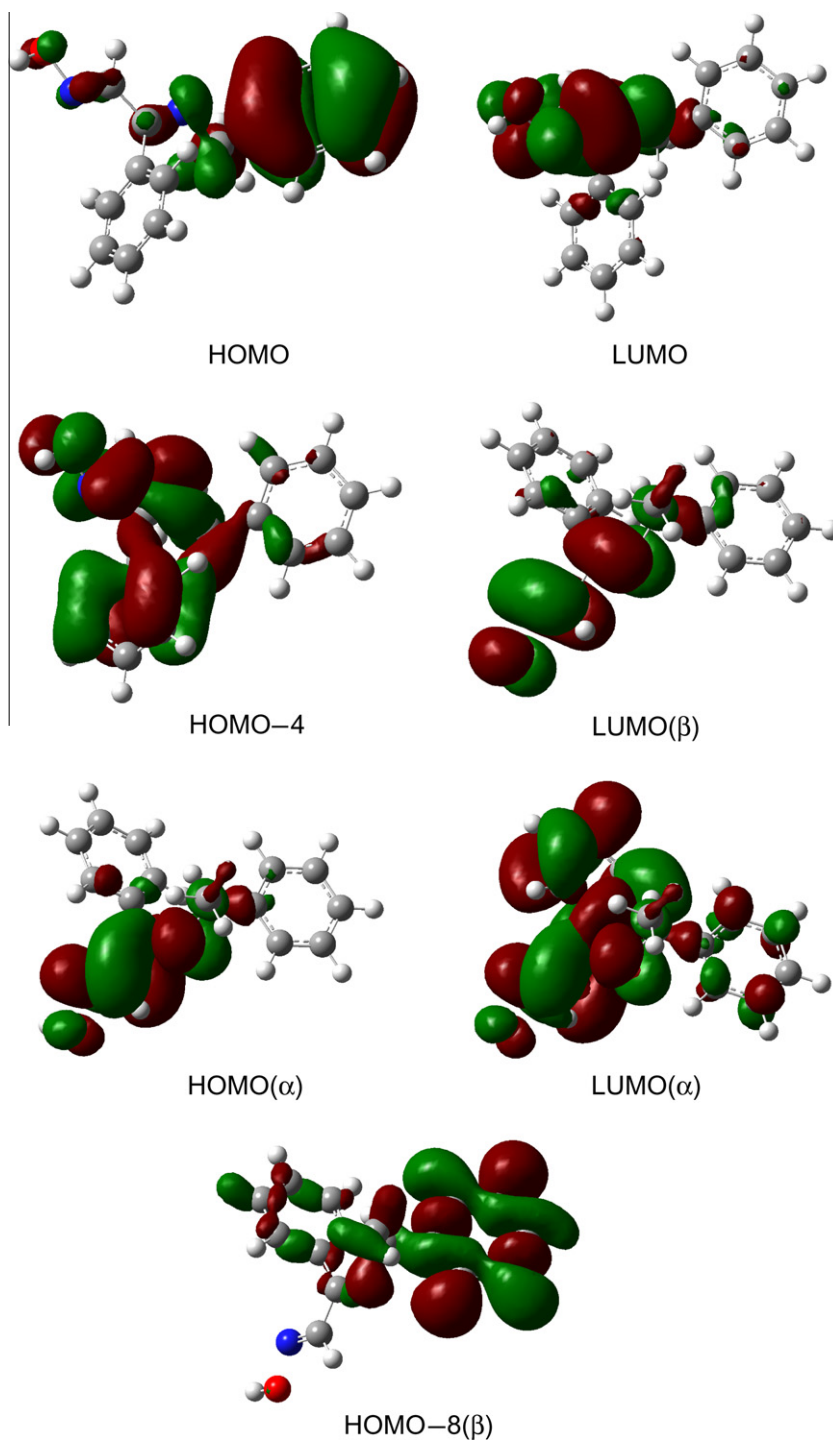


Fig. 4. The molecular orbitals involved in the electronic transitions. The α - and β -spin HOMO and LUMO orbitals indicate the triplet state of I.

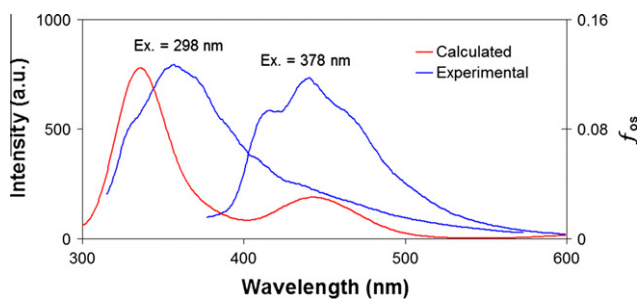


Fig. 5. Experimental and calculated emission spectra of compound I.

the nature of the electronic transitions observed in the absorption and emission spectra. The calculated geometry of the *s-trans-E,E* isomer is in good agreement with the X-ray crystallographic data and the calculated vibrational spectra and chemical shift values compare well with the experimental data. The calculated vibrational bands and NMR chemical shifts are consistent with the experimental results. The electronic absorption and emission spectra calculated using the TD-DFT method were correlated to the experimental spectra, and the assignment and analysis of the electronic transitions were performed using the frontier molecular orbitals. The absorption band is consistent with the calculated band within only 1 nm wavelength shift, while the calculated

emissions of the title compound agree well with the experimental data. The analysis of the frontier HOMO and LUMO orbitals clearly indicates that both absorption and emission bands are originated mainly from the π - π^* transitions.

Supplementary material

CCDC 869857 contains the supplementary crystallographic data for compound **I**. These data can be obtained free of charge from The Cambridge Crystallographic Data Centre via http://www.ccdc.cam.ac.uk/data_request/cif.

Acknowledgment

This work is a part of a research Project, OUAP(F-2012/12), supported by the research fund of Uludag University.

References

- [1] A. Chakravorty, *Coord. Chem. Rev.* 13 (1974) 1.
- [2] M.E. Keeney, K. Osseo-Asare, K.A. Woode, *Coord. Chem. Rev.* 59 (1984) 141.
- [3] V.Yu. Kukushkin, D. Tudela, A.J.L. Pombeiro, *Coord. Chem. Rev.* 156 (1996) 333.
- [4] V.Yu. Kukushkin, A.J.L. Pombeiro, *Coord. Chem. Rev.* 181 (1999) 147.
- [5] A.G. Smith, P.A. Tasker, D.J. White, *Coord. Chem. Rev.* 24 (2003) 61.
- [6] P. Chaudhuri, *Coord. Chem. Rev.* 243 (2003) 143.
- [7] C.J. Milios, T.C. Stamatatos, S.P. Perlepes, *Polyhedron* 25 (2006) 134.
- [8] H. Nakamura, Y. Iitaka, H. Sakakibara, H. Umezawa, *J. Antibiot.* 27 (1974) 894.
- [9] H.A. Kirst, E.F. Szymanski, D.E. Doman, J.L. Occolowitz, N.D. Jones, M.O. Chaney, R.L. Hamill, M.M. Hoehn, *J. Antibiot.* 28 (1975) 286.
- [10] V.V. Ponomareva, N.K. Halley, X. Kou, N.N. Gerasimchuk, K.V. Domasevich, *J. Chem. Soc. Dalton Trans.* (1996) 2351.
- [11] T.W. Hambley, E.C.H. Ling, S. O'Mara, M.J. McKeage, P.J. Russell, *J. Biol. Inorg. Chem.* 5 (2000) 675.
- [12] A.G. Quiroga, L. Cubo, E. de Blas, P. Aller, C.J. Navarro-Ranninger, *Inorg. Biochem.* 101 (2007) 104.
- [13] S. Zorbas-Seifried, M.A. Jakupec, N.V. Kukushkin, M. Groessl, Ch.G. Hartinger, O. Semenova, H. Zorbas, V.Yu. Kukushkin, B.K. Kepler, *Mol. Pharmacol.* 71 (2007) 357.
- [14] Y.Yu. Scaffidi-Domianello, K. Meelich, M.A. Jakupec, V.B. Arion, V.Yu. Kukushkin, M. Galanski, B.K. Kepler, *Inorg. Chem.* 49 (2010) 5669.
- [15] R. Glaser, A. Streitwieser, *J. Am. Chem. Soc.* 111 (1988) 7340.
- [16] P.G. Kolandaivel, N. Kuze, T. Sakaizumi, O. Ohashi, K. Lijima, *J. Phys. Chem. A* 101 (1997) 2873.
- [17] P. Kolandaivel, K. Senthilkumar, *J. Mol. Struct. (Theochem)* 535 (2001) 61.
- [18] P.I. Nagy, J. Kókósi, A. Gergely, A. Rácz, *J. Phys. Chem. A* 107 (2003) 7861.
- [19] I. Georgieva, N. Trendafilova, *Chem. Phys.* 321 (2006) 311.
- [20] S. Nsikabaka, W. Harb, M.F. Ruiz-López, *J. Mol. Struct. (Theochem)* 764 (2006) 161.
- [21] A.R. Bekhradnia, S. Arshadi, *Monatsh. Chem.* 138 (2007) 725.
- [22] H. Tavakol, S. Arshadi, *J. Mol. Model.* 15 (2009) 807.
- [23] A.V. Afonin, I.A. Ushakov, D.V. Pavlov, A.V. Ivanov, A.I. Mikhaleva, *Magn. Reson. Chem.* 48 (2010) 685.
- [24] J. Grzegorzec, Z. Mielke, *Eur. J. Org. Chem.* (2010) 5301.
- [25] L.D. Popov, S.I. Levchenkov, I.N. Shcherbakov, V.A. Kogan, Yu.P. Tupolova, *Russ. J. Gen. Chem.* 80 (2010) 493.
- [26] J. Jayabharathi, A. Manimekalai, M. Padmavathy, *Med. Chem. Res.* 20 (2011) 981.
- [27] F. Azarakhshi, D. Nori-Shargh, N. Masnabadi, H. Yahyaei, S.N. Mousavi, *Phosphorus, Sulfur Silicon* 187 (2012) 276.
- [28] U. Sayin, O. Dereli, E. Turkkan, A. Ozmen, *Radiat. Phys. Chem.* 81 (2012) 146.
- [29] G.P. Li, W.R. Xu, X.J. Lin, C.B. Liu, *Chem. Lett.* 17 (2006) 423.
- [30] J. Wang, J. Gu, J. Leszczynski, M. Feliks, W.A. Sokalski, *J. Phys. Chem. B* 111 (2007) 2404.
- [31] K. Sharma, S.B. Mishra, A.K. Mishra, *Helv. Chim. Acta* 94 (2011) 2256.
- [32] A.P. Guimarães, T.C.C. França, T.C. Ramalho, M.N. Rennó, E.F. Ferreira da Cunha, K.S. Matos, D.T. Mancini, K. Kuča, *J. Appl. Biomed.* 9 (2011) 163.
- [33] T. Stepanenko, L. Lapinski, M.J. Nowak, L. Adamowicz, *Vib. Spectrosc.* 26 (2001) 65.
- [34] K. Sohlberg, K.D. Dobbs, *J. Mol. Struct. (Theochem)* 577 (2002) 137.
- [35] K. Malek, M. Vala, H. Kozłowski, L.M. Proniewicz, *Magn. Reson. Chem.* 42 (2004) 23.
- [36] B. Golec, Z. Mielke, *J. Mol. Struct.* 844–845 (2007) 242.
- [37] B. Golec, J. Grzegorzec, Z. Mielke, *Chem. Phys.* 353 (2008) 13.
- [38] T. Irshaidat, *Tetrahedron Lett.* 49 (2008) 631.
- [39] N.V. Istomina, N.A. Shcherbina, L.B. Krivdin, *Russ. J. Org. Chem.* 45 (2009) 481.
- [40] V. Arjunan, C.V. Mythili, K. Mageswari, S. Mohan, *Spectrochim. Acta Part A* 79 (2011) 245.
- [41] N.R. Gonewar, V.B. Jadhav, K.D. Jadhav, R.G. Sarawadekar, *Res. Pharm.* 2 (2012) 18.
- [42] G.M. Sheldrick, *Acta Crystallogr. A* 64 (2008) 112.
- [43] A.E. Frisch, R.D. Dennington, T.A. Keith, A.B. Nielsen, A.J. Holder, *Gaussian 3.0*, Gaussian, Inc., Wallingford, USA, 2003.
- [44] M.J. Frisch, G.W. Trucks, H.B. Schlegel, G.E. Scuseria, M.A. Robb, J.R. Cheeseman, J.A. Montgomery Jr., T. Vreven, K.N. Kudin, J.C. Burant, J.M. Millam, S.S. Iyengar, J. Tomasi, V. Barone, B. Mennucci, M. Cossi, G. Scalmani, N. Rega, G.A. Petersson, H. Nakatsuji, M. Hada, M. Ehara, K. Toyota, R. Fukuda, J. Hasegawa, M. Ishida, T. Nakajima, Y. Honda, O. Kitao, H. Nakai, M. Klene, X. Li, J.E. Knox, H.P. Hratchian, J.B. Cross, V. Bakken, C. Adamo, J. Jaramillo, R. Gomperts, R.E. Stratmann, O. Yazyev, A.J. Austin, R. Cammi, C. Pomelli, J.W. Ochterski, P.Y. Ayala, K. Morokuma, G.A. Voth, P. Salvador, J.J. Dannenberg, V.G. Zakrzewski, S. Dapprich, A.D. Daniels, M.C. Strain, O. Farkas, D.K. Malick, A.D. Rabuck, K. Raghavachari, J.B. Foresman, J.V. Ortiz, Q. Cui, A.G. Baboul, S. Clifford, J. Cioslowski, B.B. Stefanov, G. Liu, A. Liashenko, P. Piskorz, I. Komaromi, R.L. Martin, D.J. Fox, T. Keith, M.A. Al-Laham, C.Y. Peng, A. Nanayakkara, M. Challacombe, P.M.W. Gill, B. Johnson, W. Chen, M.W. Wong, C. Gonzalez, J.A. Pople, *Gaussian 03*, Revision E.01, Gaussian, Inc., Wallingford, CT, 2004.
- [45] A.D. Becke, *J. Chem. Phys.* 98 (1993) 5648.
- [46] N. Sundaraganesan, S. Illakiamani, H. Saleem, P.M. Wojciechowski, D. Michalska, *Spectrochim. Acta* 61A (2005) 2995.
- [47] A.J.L. Jesus, M.T.S. Rosado, I. Reva, R. Fausto, M.E. Eusebio, J.S. Redinha, *J. Phys. Chem. A* 110 (2006) 4169.
- [48] K. Wolinski, J.F. Hinton, P. Pulay, *J. Am. Chem. Soc.* 112 (1990) 8251.
- [49] N.M. O'Boyle, A.L. Tenderhold, K.M. Langner, *J. Comput. Chem.* 29 (2008) 839.
- [50] P. Politzer, J.S. Murray, *The Chemistry of Hydroxylamines, Oximes and Hydroxamic Acids*, Wiley, West Sussex, 2009.
- [51] A. Yilmaz, B. Taner, P. Devci, A. Yilmaz Obali, U. Arslan, E. Sahin, H.I. Ucan, E. Ozcan, *Polyhedron* 29 (2010) 2991.
- [52] F. Piron, N. Vanthynne, B. Joulin, *J. Org. Chem.* 74 (2009) 9062.
- [53] P. Salvadori, C. Rosini, L. Di Bari, *Conformation and chiroptical properties of dienes and polyenes*, in: Z. Rappoport (Ed.), *The Chemistry of Dienes and Polyenes*, vol. 1, John Wiley & Sons, New York, 1997 (Chapter 4).
- [54] W. Danchura, R.E. Wasylshen, J. Delikatny, M.R. Graham, *Can. J. Chem.* 57 (1979) 2135.
- [55] A. Andrzejewska, L. Lapinski, I. Reva, R. Fausto, *Phys. Chem. Chem. Phys.* 4 (2002) 3289.
- [56] A.E. Reed, R.B. Weinstock, F. Weinhold, *J. Chem. Phys.* 83 (1985) 735.
- [57] A.E. Reed, L.A. Curtiss, F. Weinhold, *Chem. Rev.* 88 (1988) 899.
- [58] N. Tosa, A. Bende, R.A. Varga, A. Terec, I. Bratu, I. Grosu, *J. Org. Chem.* 74 (2009) 3944.
- [59] D.J. Giesen, N. Zumbulyadis, *Phys. Chem. Chem. Phys.* 4 (2002) 5498.
- [60] A. El Molcef, E. Zaballos, R.J. Zaragoza, *Tetrahedron* 67 (2011) 3677.
- [61] S.M. Polson, R. Cini, C. Pifferi, L.G. Marzilli, *Inorg. Chem.* 36 (1997) 314.
- [62] E. Canpolat, A. Yazıcı, M. Kaya, *J. Coord. Chem.* 60 (2007) 473.